Lumped 50-Ω Arrays of SNS Josephson Junctions

Nicolas Hadacek, Paul D. Dresselhaus, and Samuel P. Benz, *Senior Member, IEEE*

***Abstract*—For the first time, lumped series arrays of Josephson junctions have been fabricated with a transmission line-matched 50-Ω resistance. These arrays also have the thousands of junctions necessary to produce a metrologically significant voltage. This approach is expected to increase the output voltage per array and to optimize their performance for Josephson voltage standards. Traditional Josephson arrays for voltage standards have used distributed microwave structures, where array lengths are several multiples of the driving wavelength. The lumped arrays in this work have physical lengths shorter than a quarter of the microwave drive wavelength and total normal-state resistances nearly equal to the transmission line impedance. Fabrication of these arrays was made possible by use of a newly developed Nb–($MoSi_2$–Nb)$_n$ stacked junction technology. We present measurements of the microwave response of lumped arrays with total normal resistances up to 54 Ω and with various termination resistances. A simple numerical model is presented that accounts for the spatial distribution of the microwave current and for the nonuniformity of the junction critical currents. The resulting simulations agree well with experimental results.**

***Index Terms*—Josephson junctions, lumped element microwave circuits, stacked junctions, voltage standard.**

I. Introduction

THE major limitation for Josephson voltage standards has always been the small voltage of constant-voltage Shapiro steps from a single microwave-irradiated Josephson junction. Large series arrays of Josephson junctions are required to produce practical voltages. For direct current (dc) applications, an array of N junctions biased with a microwave frequency f has the first constant-voltage step at $V = N\Phi_0 f$, where $\Phi_0 = h/2e = 2.07$ μV/GHz is the quantum of magnetic flux. Presently, Josephson voltage standards (JVSs) use distributed arrays in which the total length of the array is multiple wavelengths of the microwave drive signal [1], [2]. The array length is set by the minimum line-width of the fabrication technology, the junction size, and the number of junctions required to generate a practical voltage over a usable current range (typically larger than 1 mA for the National Institute of Standards and Technology (NIST) programmable and alternating current (ac) JVS systems). Our longest distributed array of 4400 junctions driven at 18.5 GHz produces a 0.17 V constant-voltage step with 3-mA current margins [3]. With 8 μm spacing per junction, the total length of this array is 35.2 mm, which is about five times the 7.25-mm microwave drive wavelength.

The current range of the steps is degraded by both junction nonuniformity and microwave attenuation caused by junction dissipation. In conventional JVS circuits, arrays of highly capacitive superconductor–insulator–superconductor (SIS) junctions have little dissipation, and thus negligible microwave attenuation such that many junctions can be connected in series to increase the voltage per array. In contrast, programmable voltage standards require nonhysteretic junctions such as superconductor–normal metal–superconductor (SNS) junctions or superconductor–insulator–normal metal–insulator–superconductor (SINIS) junctions. In order to get the high-current densities required for large current margins and the low characteristic voltages required for pulse-driven applications, NIST has chosen to concentrate its efforts on SNS arrays.

In the case of SNS junctions, the total length of an array is usually limited by its total normal resistance since the junctions are more dissipative and thus lead to significant microwave attenuation [4]. With a few milliohms per junction for a typical normal-state resistance, these SNS arrays are limited to several thousand junctions before the total array resistance is comparable to the transmission line impedance. Arrays with more junctions or higher resistance lead to smaller operating margins because the microwave power at the end of the array decreases exponentially with the total number of junctions.

In order to achieve the largest current range in a Josephson array, each junction should have the same critical current and should receive the same amount of microwave power. The overall response of the array is optimal if the current range of the first constant-voltage step is the same for each junction. Hence, there are two design goals for optimizing the operating margins of a series array. The first goal is to fabricate uniform junctions with very similar characteristics. Thus, the fabrication process should be optimized to give uniform normal resistance R_n (determined by the junction barrier thickness and resistivity), and uniform critical currents I_c (determined by the junction area and barrier thickness). The second goal is to design the on-chip microwave coupling circuit to ensure the most uniform distribution of the microwave power along the array. If the junctions have a negligible influence on the distribution of microwave current in the coplanar waveguide (CPW) in which they are embedded, and in particular, if the microwave attenuation is negligible, it is easy to properly terminate the array by matching the termination resistance with the impedance of the waveguide. Proper termination eliminates reflections and standing waves that contribute to nonuniform power distribution along the array. The CPW characteristic impedance is usually 50 Ω to match the off-chip microwave circuitry.

Recent developments in voltage standards are challenging this simple design. First, there is a desire to increase the output voltage above 1 V for the dc programmable JVS. This can be achieved by adding more junctions per array, typically by using stacked junctions [3]. For example, a triple-stacked junction array of 4400 stacks with the same junction and design parame-

Manuscript received May 5, 2006; revised July 20, 2006. This work was supported by the Office of Naval Research under Contract N0001405IP20017 and N0001406IP20005. This paper was recommended by Associate Editor O. Mukhanov.

The authors are with the National Institute of Standards and Technology (NIST), Boulder, CO 80305 USA (e-mail: hadacek@boulder.nist.gov).

Digital Object Identifier 10.1109/TASC.2006.883456

ters described above produces 0.5 V with 1-mA current margin. These long arrays with more junctions have total resistances (55Ω for the triple stacked arrays) that are comparable to the waveguide characteristic impedance. At these resistances, these arrays have significant microwave attenuation.

Second, the arrays used in the ac Josephson voltage standard require broadband microwave response. Unlike dc JVS circuits that are designed to work at a fixed excitation frequency, the ac JVS is driven with a broadband microwave drive signal [5]. Furthermore, it is desirable to reduce the parasitic inductance between the junctions to minimize undesirable inductive voltage signals, and to remove common mode voltages associated with termination resistances. Our recently developed technology for stacked Josephson junctions enables us to fabricate arrays with high junction density to address some of these challenges [6].

It has been proposed that grounded 50-Ω lumped arrays, which are much shorter than the microwave wavelength, will have better total performance than distributed arrays for both dc and ac JVS applications [7], [8]. We note that lumped arrays of Josephson junctions were previously proposed for broadband tunable Josephson oscillators [7], while short low-resistance grounded lumped arrays are presently in use as quantum voltage noise sources for Johnson noise thermometry [9].

In this paper, we present measurements of lumped Josephson junction arrays of total resistance up to 54 Ω, and we compare those measurements to a model that combines the microwave and Josephson properties of these arrays.

II. Fabrication and Measurements

Because the first constant-voltage step has the largest amplitude, SNS-based voltage standards commonly use it to obtain the best operating margins. Due to the junction dynamics, the current ranges of the constant-voltage steps are functions of the driving microwave frequency. Arrays are typically driven at frequencies close to the junction characteristic frequency $f_c = I_c R_n/\Phi_0$, because both the amplitude of the first constant-voltage step and its immunity to junction nonuniformity are optimized in this frequency range [10]–[12]. For these measurements, the microwave power of the driving signal is optimized for the best operating margin at each frequency point to compensate for any frequency dependence of the measurement apparatus. Measuring the amplitude of the first constant-voltage step as a function of the microwave frequency is important in order to evaluate the broadband response of the array and to find the optimal operating frequencies.

This experiment investigated arrays of lengths l_A shorter than a quarter of the microwave wavelength at the junction characteristic frequency and with total normal resistances, $R_A = R_n N$ (for N junctions in the array) up to 50 Ω. These two prerequisites impose a constraint on the maximum critical current of the junctions [7]. Critical currents around 10 mA are usually optimal for voltage standards with large operating margins because of the smaller junction resistance, and thus lower microwave attenuation. Such design balances the microwave attenuation with the amount of available microwave power needed to drive the array. The large critical currents also result in large current steps of a few milliamperes that enhance the noise immunity and operating range of the arrays.

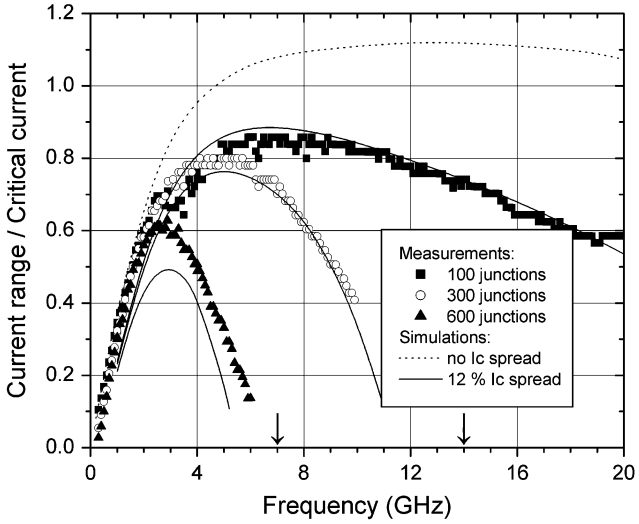

Fig. 1. Normalized current range of the first Shapiro step versus microwave frequency for arrays of 100, 300, and 600 nonstacked junctions terminated by a short to ground. Arrays are 0.8-, 2.4-, and 4.8-mm long, respectively. Symbols are measured data. The step vanishes when the quarter-wavelength nears the array length at 35, 14, and 7 GHz, respectively (as indicated by arrows on the graph). Dotted line corresponds to a simulation of a 0.8-mm-long array, assuming no spread in critical currents. Solid lines indicate simulations of the three different array lengths with a 12% spread in critical currents.

At the characteristic frequency, and for an array shorter than a quarter-wavelength, the critical current is constrained such that

$$I_c < \frac{c\Phi_0}{4\sqrt{\varepsilon_r}} \frac{n}{aR_A} \tag{1}$$

where c is the speed of light, n is the number of junctions per stack, ε_r is the effective permittivity coefficient of the transmission line, and a is the spacing between stacks. For eight junctions per stack, a spacing of 8 μm, and $R_A = 50\ \Omega$, this gives a maximum critical current of 1.4 mA. Fabrication of junctions with such low critical currents was accomplished by means of both smaller junction areas (4 $\times$ 4 μm) and thicker $MoSi_2$ barriers (25.2 nm) compared to our regular design. This gives characteristic voltages near 10 μV, corresponding to characteristic frequencies around 4.8 GHz.

Short arrays of both nonstacked and stacked junctions have been fabricated and measured. This allows differentiation between the effects of an imperfect termination and of high junction density. Our fabrication technology for arrays of junctions with $MoSi_2$ barriers has been described previously [6]. Although stacks of up to 10 junctions have been demonstrated, we chose to make stacks of only eight junctions to improve the junction uniformity.

First, we fabricated series arrays of nonstacked planar junctions with 100, 300, and 600 series junctions; their total lengths are, respectively, 0.8, 2.4, and 4.8 mm. These arrays are terminated by a short to the ground of the coplanar waveguide. Fig. 1 shows the normalized amplitude of the first constant-voltage step of these three arrays as a function of the driving microwave frequency.

For the two longest arrays, the current range decreases to zero near the frequency at which the quarter-wavelength equals the array length. This is expected because the microwave current,

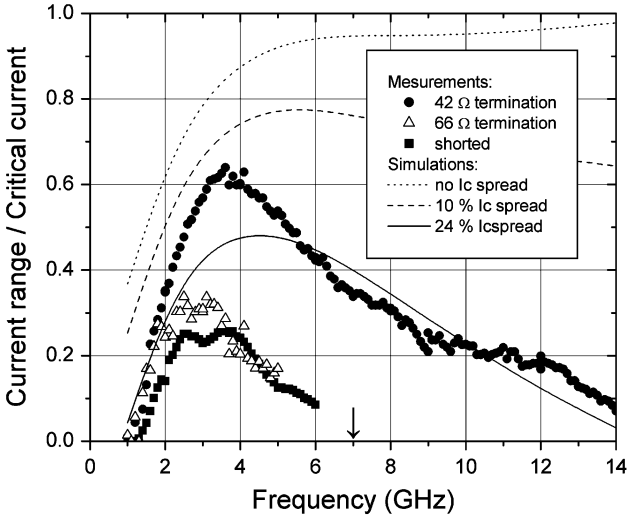

Fig. 2. Normalized current range of the first Shapiro step versus microwave frequency for 600-stack arrays. Symbols are measurements for three arrays with different terminations: a short to ground, a 42-Ω resistor, and a 66-Ω resistor. All three arrays are nominally identical, with 600 stacks of eight junctions each fabricated on the same wafer. Total normal resistance is 54 Ω. Lines are simulations for 4.8-mm-long arrays with a 50-Ω normal resistance, a 40-Ω termination resistor, and different spreads in critical current. Arrow indicates the frequency where the microwave quarter-wavelength equals the array length.

which is reflected at the shorted end, has a node at a distance of one quarter-wavelength from the end. At higher frequencies, this node resides within the array, and the junctions positioned near the node have a vanishing microwave current. In the shortest, 100-junction array, the step size peaks around the junction characteristic frequency, $f_c \approx 5$ GHz, because at this point the array is the least sensitive to variations in the junction parameters [10]–[12]. The gradual decrease of the step size at higher frequencies can be qualitatively explained by the gradual encroachment of the microwave current node at the drive end of the array. For the longest arrays, this rollover occurs for $f < f_c$, and thus decreases the current range, even at the characteristic frequency.

Arrays were also fabricated with 100, 300, and 600 stacks with eight junctions per stack by use of the same lithographic masks as the previously described arrays of nonstacked junctions. We focus on the circuits with arrays of 600 stacks in order to evaluate the transmission line effects that are most prominent in these longer arrays. These 600-stack arrays contain 4800 junctions each and have a normal-state resistance of 54 Ω.

Arrays terminated with different resistances R_T, a short, a 42-Ω resistor, and a 66-Ω resistor, are compared. Fig. 2 shows the measured current range versus frequency of the arrays for these different terminations. The on-chip termination resistors are fabricated with a variable length dc-sputtered PdAu film. These resistors are less than 300-μm-long, so they are effectively lumped at the frequencies considered in this study. The circuit with the 42-Ω termination resistor has the largest current range, indicating that this circuit produces the best microwave uniformity across the array. Both the shorted array and the array with a 66-Ω termination have smaller current ranges. Qualitatively we note that the large total resistance of the arrays significantly modifies the spatial distribution of microwave current because there is microwave attenuation from the junctions as well as a reflection at the end of the transmission line due to imperfect termination. In this case, finding the termination that gives the largest current range is not trivial.

III. Modeling

A lumped 50-Ω array should effectively terminate the transmission line and produce no reflections. But our arrays have a nonnegligible length, and even a quarter-wavelength 50-Ω resistor will not produce a perfect termination, due to its distributed geometry leading to reflections and to distributed capacitance and inductance. Furthermore, the junctions in these arrays have nonlinear electrical characteristics.

There are two aspects of the Josephson junction arrays that need to be modeled, namely the distribution of microwave current amplitude along the array, and the response of an individual junction in the array to the local microwave current amplitude. The microwave distribution will depend on the microwave frequency, the array length, the total resistance, and the termination of the array. The constant-voltage step current range of a single junction in the array depends on the microwave frequency normalized by the junction characteristic frequency, and on the microwave current amplitude normalized by the junction critical current. With our present circuit designs, it is not possible to directly measure either the distribution of microwave current or the current range of an individual junction. Thus, we can measure only the aggregate current range of the whole array at a given microwave frequency and power.

To describe the distribution of the microwave signal along the array, we model the CPW in which the array is embedded as a nondispersive transmission line characterized by a linear inductance L, and a linear capacitance C. Since we are using superconducting transmission lines, we assume that the microwave drive to the array is supplied by an infinite nonresistive CPW with $L = 0.37$ pH/μm and $C = 0.15$ fF/μm with a 50-Ω characteristic impedance and an effective permittivity of 5 (the electromagnetic field is half in air and half in the silicon wafer which has a relative permittivity of about 11). The segment of CPW containing the array is lossy with a linear resistance R given by the normal resistance of the array R_A divided by its length l_A. As a simplification the junction influence on the microwave signal is considered to be only that of a distributed resistor, so that the values for L and C for this segment are identical to those of the CPW. The effects of the nonlinear Josephson dynamics on the microwave distribution in the array, such as the reactance of the junctions, are ignored.

The microwave signal is modeled by incoming and reflected transverse electromagnetic (TEM) waves for current and voltage with a continuity condition between adjacent segments and a boundary end-condition set by the termination resistor R_T. On each segment i with angular frequency ω, the series impedance per unit length Z_i, the shunt admittance per unit length Y_i, and the voltage $V_i(z,t)$ at position z and time t are given by

$$\begin{aligned} Z_i &= R_i + j\omega L_i \\ Y_i &= j\omega C_i \\ V_i(z,t) &= V_{0,i}^{+} e^{-\sqrt{Z_i Y_i} z + j\omega t} + V_{0,i}^{-} e^{\sqrt{Z_i Y_i} z + j\omega t}. \end{aligned}$$

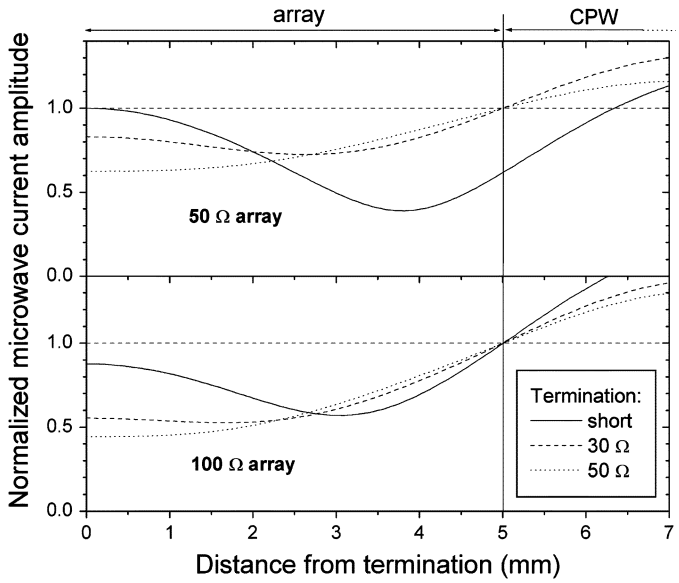

Fig. 3. Simulations of 8-GHz microwave current amplitude along a 5-mm-long array for three different terminations: short to ground, 30 Ω, and 50 Ω. The upper (lower) panel is calculated for an array of total normal resistance 50 Ω (100 Ω). Magnitude of the current is normalized to the maximum amplitude inside the array.

The microwave power applied to the array, but not the distribution within the array, is dependent on the external microwave circuit. In this model, adding a resistor on the input side of the array will not modify the functional distribution of microwave current along the array. However, such a design reduces reflections between the array and the microwave generator, and thus suppresses standing wave variations in the microwave power caused by these reflections. These standing wave oscillations of the microwave power have been observed in arrays terminated by a short and are due mostly to the imperfect termination. They may alternatively be damped by inserting microwave attenuators between the generator and the array.

Fig. 3 shows examples of a simulation for 50-Ω and 100-Ω arrays with different termination resistances. At the chosen frequency (8 GHz) and array length (5 mm), the microwave current amplitude has the best spatial uniformity for a 30-Ω termination with a 50-Ω array, and for a short-circuit termination with a 100-Ω array. The spatial uniformity is optimized because the power reflected at the nonmatching termination partially compensates for the losses along the resistive transmission line. We also note that the microwave current variation is 40% for the short-terminated 100-Ω array and 25% for the 30-Ω -terminated 50-Ω array, so that the array of lower impedance has better overall current uniformity.

To compute the current ranges of the constant-voltage steps for the entire array, the details of the microwave current amplitude distribution are not important; knowing the relative difference between the minimum and maximum amplitudes is sufficient because only the junctions positioned at these current values constrain the total current range. All the other junctions, assuming identical junction characteristics, will have steps situated between these extremes.

For a termination that does not match the CPW impedance, the best broadband performance will be realized by having the array immediately adjacent to the termination. Indeed, the principal limitation of step range is due to the first minimum of microwave current amplitude. The frequency at which this first minimum lands inside the array will be higher for an array adjacent to the termination. However, this is not the case if the design goal is to get the largest current step at a fixed frequency for which the positions of the nodes can be computed. Therefore, one way to further optimize the fixed-frequency array performance would be to place the array or sections of the array between minima of the microwave current amplitude. A similar approach was demonstrated for distributed series-array Josephson oscillators [13], [14].

The second part of the model is to compute the current–voltage (I–V) characteristics of an SNS junction biased with a microwave current. Here, we use the resistively shunted junction (RSJ) model, which accounts for the nonlinear junction dynamics. The measured I–V curves for our $MoSi_2$ junctions are similar to those predicted by this model for characteristic voltages near 50 μV [15]. At lower characteristic voltages, as with the junctions presented here, I–V curves deviate from the RSJ model and show excess current. This is not taken into account in our model. The evolution of the junction phase with time using the Josephson equations is numerically computed. The voltage across the junction is then the time average of the phase derivative. Using this model, we obtain plots of the array current range versus microwave current amplitude at different frequencies.

It is straightforward to combine the spatial distribution of microwave current amplitudes and the current range dependence on the microwave current. For a given microwave power, the overlap of the current ranges at the maximum and minimum microwave current amplitude gives the net current range for the entire array. Just as the microwave power at each frequency is tuned during measurements to give the maximum current range for the first constant-voltage step, this same procedure is followed for the numerical calculations.

Our model calculates the maximum current range versus frequency for a given array circuit design (characteristic voltage, array length, number of junctions, and termination resistance). Using only these parameters, the simulations do not agree well with our measurements. Up to this point, we have not accounted for any spread in critical currents, but have assumed that all the junctions could be considered identical. Practically, the fabrication process always results in a spread in effective junction area. This could be caused by some combination of imperfect lithographic masks, nonuniform junction etching, and, for stacked junctions, nonvertical etch profiles and irreproducible barriers. Even a relatively small spread in critical currents induces a significant decrease of the overall current range of the constant-voltage step for an array. As illustrated in Fig. 4, a nonidentical critical current shifts the center of the step current range and also varies the optimal microwave current amplitude that gives the maximum current range for that particular junction. It should be noted that the nonuniformities contribute not as a variance of a statistical distribution of critical currents, but as its absolute extremes.

With no distribution of microwave current, only the extreme junctions are important for calculating the step size; otherwise,

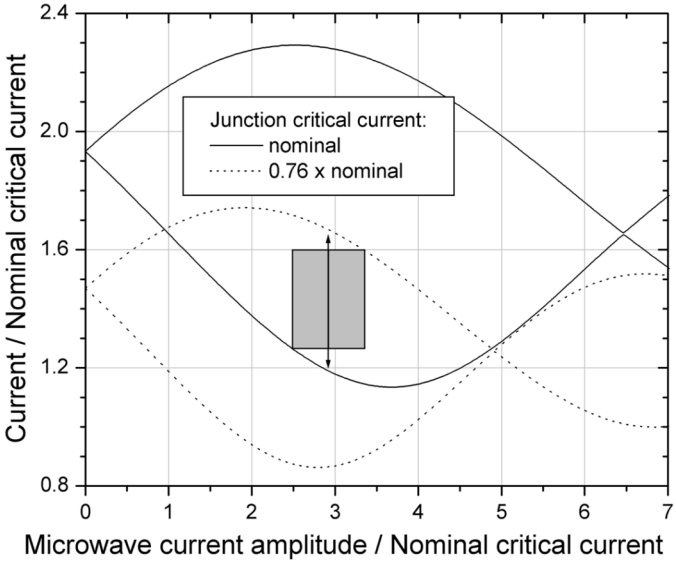

Fig. 4. Simulations of the first Shapiro step as a function of the microwave current amplitude for junctions with a 10-μV characteristic voltage driven at 8 GHz. Solid lines are the upper and lower edges of the step for a junction with nominal critical current. Dotted lines are for a junction with a 24% smaller critical current. Maximum current range that can be obtained for a single stack in an array with a 24% spread in critical currents is indicated by arrows. Height of the grayed box corresponds to the maximum current range for the same array with a nonuniform microwave distribution. Box width is the span of microwave current amplitudes along the array for a relative span of 0.25, which is the value computed for a 5-mm-long 50-Ω array terminated by a 30-Ω resistor.

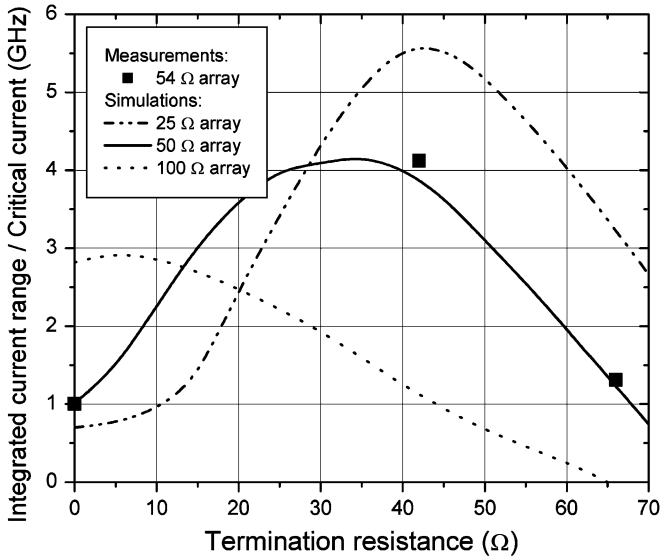

Fig. 5. Current range integrated over the frequency range where steps are larger than 10% of the critical current, as a function of termination resistance. Squares correspond to measured steps for the three 4.8-mm-long arrays presented in Fig. 2. Lines are simulations for 4.8-mm-long arrays with normal resistances of 25, 50, and 100 Ω, and a 24% spread in critical currents.

the distribution of junction critical currents, as well as the distribution of microwave current, must be included. The spread in critical currents is assumed to be uniform along the array; this simplification means that at each position there is one junction with the minimum critical current and another with the maximum critical current. This hypothesis correctly describes the spread due to nonvertical etch profiles for stacked junctions, which is likely to be our dominate source of junction nonuniformity. SEM micrographs show that the junction at the top of each stack has a smaller area than the junction at the bottom. However, this spread model cannot account for location-dependent effects during processing, such as loading of the etching plasma, which could shrink the junction size at the ends of an array. Fig. 4 also illustrates the effect on the current range of a spread in critical currents and of a nonuniform microwave distribution.

Fig. 1 also shows a comparison of our model with the measured current range versus frequency for shorted arrays of non-stacked junctions. The 10-μV junction characteristic voltage is fixed by the barrier deposition, so the only free parameter for our model is this critical current spread expressed as a percentage of nominal critical current. We use a 12% spread in critical current to account for the roll-off of the 100 junction array. For simulations made with and without microwave dissipation, the current ranges are within 5% of each other. The simulations have been made with the measured normal resistances of each array (this resistance is 6.3 Ω for the 600-junction array). The simulations agree well with the measurements, except for the longest 600-junction array, for which the simulation underestimates the current range. Our model tends to underestimate the current step size close to the characteristic junction frequency (between 2 and 5 GHz). The reason for this may be due to dynamic junction impedance effects [16] not included in our model. These effects are greater at frequencies lower than the junction characteristic frequency.

In addition, Fig. 2 shows measured step heights versus frequency for a 600 stack array with a 42-Ω termination compared to our model for different amounts of critical current nonuniformity. A 24% spread gives the best agreement for stacked arrays. It should be noted that, in addition to the critical current nonuniformity, this large spread may also include a spread in bias current due to electrical noise.

Some criterion is needed to easily compare different circuit designs. Such a criterion could be the maximum step size. Another criterion that reflects the overall broadband properties of each array is the current range integrated over frequency. An example of this criterion is plotted in Fig. 5. Because our critical current measurements are less accurate below 0.1 mA, we considered only the frequency range where steps are larger than 10% of the critical current. Fig. 5 allows comparison of 4.8-mm-long arrays that have different normal resistances and different termination resistances, and with a 24% spread in critical currents. The optimal calculated termination resistance for 25-, 50-, and 100–Ω arrays are respectively close to 42, 35, and 5 Ω. Those values correspond roughly to the terminations found in Fig. 3 that give the most uniform microwave current distribution at a given frequency. Measured current ranges for the three arrays presented in Fig. 2 are very close to the simulated curve for the chosen criterion.

IV. Conclusion

Using Nb–($MoSi_2$–Nb)$_n$ stacked junctions we fabricated and measured SNS arrays whose normal-state resistances were comparable to the transmission line impedance, while keeping the total lengths of the array less than a quarter-wavelength at the junction characteristic frequency. We used a lossy-transmission

line model to simulate the current range of constant-voltage steps for these arrays. Junction nonuniformity was added to the model in order to achieve agreement with the measurements. These results can now be used both as a diagnostic to improve our fabrication and as a basis to design more advanced voltage standards and other SNS junction circuits using lumped arrays.

ACKNOWLEDGMENT

The authors would like to thank C. Burroughs and B. Baek for measurement assistance and J. Booth and C. Reintsema for helpful comments.

REFERENCES

[1] J. Niemeyer, *Handbook of Applied Superconductivity*. Philadelphia, PA: Bernd Seeber, Inst. Phys., 1998, vol. 2, p. 1813.
[2] C. A. Hamilton, "Josephson voltage standards," *Rev. Sci. Instrum.*, vol. 71, pp. 3611–3623, Oct. 2000.
[3] Y. Chong, C. J. Burroughs, P. D. Dresselhaus, N. Hadacek, H. Yamamori, and S. P. Benz, "Practical high-resolution programmable Josephson voltage standards using double- and triple-stacked MoSi2-barrier junctions," *IEEE Trans. Appl. Supercond.*, vol. 15, no. 2, pp. 462–464, Jun. 2005.
[4] S. P. Benz and C. A. Hamilton, "Application of the Josephson effect to voltage metrology," *Proc. IEEE*, vol. 92, no. 10, pp. 1617–1629, Oct. 2004.
[5] S. P. Benz, C. J. Burroughs, and P. D. Dresselhaus, "AC coupling technique for Josephson waveform synthesis," *IEEE Trans. Appl. Supercond.*, vol. 11, no. 2, pp. 612–616, Jun. 2001.
[6] N. Hadacek, P. D. Dresselhaus, Y. Chong, S. P. Benz, and J. E. Bonevich, "Fabrication and measurement of tall stacked arrays of SNS Josephson junctions," *IEEE Trans. Appl. Supercond.*, vol. 15, no. 2, pp. 110–113, Jun. 2005.
[7] R. H. Ono and S. P. Benz, "Optimum characteristics of high temperature Josephson junctions for "lumped" array applications," in *Extended Abstracts 7th Int. Superconductive Electron. Conf. (ISEC'99)*, 1999, pp. 301–303.
[8] S. P. Benz, P. D. Dresselhaus, and C. J. Burroughs, "Nanotechnology for next generation Josephson voltage standards," *IEEE Trans. Instrum. Meas.*, vol. 50, no. 6, pp. 1513–1518, Dec. 2001.
[9] S. P. Benz, P. D. Dresselhaus, and J. Martinis, "An ac Josephson source for Johnson noise thermometry," *IEEE Trans. Instrum. Meas.*, vol. 52, no. 2, pp. 545–549, Apr. 2003.
[10] R. L. Kautz, "Shapiro steps in large-area metallic-barrier Josephson junctions," *J. Appl. Phys.*, vol. 78, pp. 5811–5819, Nov. 1995.
[11] S. I. Borovitskii, A. M. Klushin, T. B. Korotina, A. E. Pariiskii, S. K. Khorshev, and P. A. Shisharin, "Increasing the working voltage across chains of Josephson junctions," *Sov. Tech. Phys. Lett.*, vol. 11, pp. 275–277, Jun. 1985.
[12] S. P. Benz and C. J. Burroughs, "Constant-voltage steps in arrays of Nb-PdAu-Nb Josephson junctions," *IEEE Trans. Appl. Supercond.*, vol. 7, no. 2, pp. 2434–2436, Jun. 1997.
[13] K. Wan, A. K. Jain, and J. E. Lukens, "Submillimeter wave generation using Josephson arrays," *Appl. Phys. Lett.*, vol. 54, pp. 1805–1807, May 1989.
[14] P. A. A. Booi and S. P. Benz, "High power generation with distributed Josephson-junction arrays," *Appl. Phys. Lett.*, vol. 68, pp. 3799–3801, Jun. 1996.
[15] Y. Chong, P. D. Dresselhaus, and S. P. Benz, "Electrical properties of Nb-MoSi2-Nb Josephson junctions," *Appl. Phys. Lett.*, vol. 86, p. 232505, 2005.
[16] F. Auracher and T. Van Duzer, "RF impedance of superconducting weak links," *J. Appl. Phys.*, vol. 44, pp. 848–851, Feb. 1973.

Nicolas Hadacek was born in Amiens, France, on November 22, 1974. He received the engineer degree with specialization in physics from Ecole Centrale Paris, Paris, France, in 1997, and the predoctoral degree in condensed matter physics from Orsay Universitiy, Paris, France, and Jussieu University, Paris, France, the following year. He received the Ph.D. degree from Joseph Fourier University, Grenoble, France, in 2002, for his work at Commissariat à l'Energie Atomique on thin films and Josephson junctions made of superconducting nitrites.

Since 2003, he has been a Guest Researcher with the Quantum Voltage Project at the National Institute of Standards and Technology (NIST), Boulder, CO. His work is mainly focused on fabricating stacked Josephson junctions and lumped arrays for voltage standards.

Paul D. Dresselhaus was born on January 5, 1963 in Arlington, MA. He received degrees in both physics and electrical engineering from the Massachusetts Institute of Technology (MIT), Cambridge, in 1985, and the Ph.D. degree in applied physics from Yale University, New Haven, CT, in 1991.

In 1999, he joined the Quantum Voltage Project at the National Institute of Standards and Technology (NIST), Boulder, CO, where he has developed novel superconducting circuits and broadband bias electronics for precision voltage waveform synthesis and programmable voltage standard systems. For over three years at Northrop Grumman, he designed and tested numerous gigahertz speed superconductive circuits, including code generators and analog-to-digital converters. He also upgraded the simulation and layout capabilities at Northrop Grumman to be among the world's best. His previous work as a postdoctoral assistant at the State University of New York (SUNY), Stony Brook focused on the nanolithographic fabrication and study of Nb–AlOx–Nb junctions for single electron and SFQ applications, single electron transistors and arrays in Al-AlOx tunnel junctions, and the properties of ultra-small Josephson junctions.

Samuel P. Benz (SM'00) was born in Dubuque, IA, on December 4, 1962. He majored in both physics and mathematics at Luther College, Decorah, IA, where he graduated *summa cum laude* with the B.A. degree in 1985. He was awarded an R. J. McElroy fellowship (1985–1988) to pursue the Ph.D., and received the M.A. and Ph.D. degrees in physics from Harvard University, Cambridge, MA, in 1987 and 1990, respectively.

In 1990, he began working at the National Institute of Standards and Technology as a NIST/NRC Postdoctoral Fellow and joined the permanent staff in January 1992. He has been Project Leader of the Quantum Voltage Project at NIST since October 1999. He has worked on a broad range of topics within the field of superconducting electronics, including Josephson junction array oscillators, single flux quantum logic, ac and dc Josephson voltage standards, and Josephson waveform synthesis. He has 105 publications and three patents in the field of superconducting electronics.

Dr. Benz is a member of Phi Beta Kappa and Sigma Pi Sigma. He received the U.S. Department of Commerce Gold Medal for Distinguished Achievement.